Parameters of Dynamic and Static Iodine-123-MIBG Cardiac Imaging

Ali S. Arbab, Kiyoshi Koizumi, Hajime Takano, Guio Uchiyama, Takao Arai and Keisuke Mera

Department of Radiology and the Second Department of Internal Medicine, Yamanashi Medical University, Tamaho-cho, Nakakoma-gun, Yamanashi-ken, Japan

Dynamic and static ^{123}I-MIBG studies were used to investigate various parameters with regard to their usefulness in evaluating cardiac disorders. **Methods:** Four patient groups and one control group were included in this study. Dynamic study was acquired immediately after injection at 1 frame/sec for 2 min and at 1 frame/6 sec for the next 30 min using a 64 × 64 matrix format. Static study consisted of planar images at the anterior and left anterior oblique 45° views in a 512 × 512 matrix format for 1 min. The early and delayed planar images were acquired soon after dynamic acquisition and approximately 4 hr after injection, respectively. Net injection dose was calculated as the difference in syringe counts before and after injection. From the dynamic and static studies, the heart uptake ratios at 3 min and 30 min, early uptake ratio and delayed uptake ratio were calculated at various intervals. Early and delayed clearance rates, K_e and K_d, respectively were also determined. These parameters were compared and correlated with each other. **Results:** Three-minute heart uptake ratios were significantly higher than early or delayed uptake ratios or uptake ratios at 30 min in all groups. All uptake ratios in hemodialysis patients were significantly higher than those in other groups. The K_d values in dilated cardiomyopathy, doxorubicin therapy and vasospastic angina patients were significantly higher than those in hemodialysis patients and normal controls. At least bi-exponential clearance patterns of MIBG from the heart were observed in all groups. **Conclusion:** Three-minute and delayed heart uptake ratios calculated from dynamic and static studies are helpful in elucidating the uptake at nonvesicular sites, which reflect the severity of sympathetic nervous system abnormalities in the heart.

Key Words: cardiomyopathy; iodine-123-MIBG; heart uptake ratio; heart clearance rate; sympathetic function; angina

J Nucl Med 1995; 36:962–968

The sympathetic nervous system (SNS) plays an important role in regulating cardiac function in the normal and disease states (*1*). Abnormal function of the SNS is seen in various cardiac diseases and especially in cardiomyopathy (*2–4*). The blood norepinephrine level is increased in patients with end-stage renal failure on hemodialysis and in patients with chronic renal failure. This increase may be due either to a hyperactive SNS or to reduced renal clearance (*5,6*). There are also reports that inhibition of sympathetic function plays a major role in the development of vasospastic angina (*7*).

Metaiodobenzylguanidine (MIBG), an analog of the false neurotransmitter guanithidine, is known to be taken up and stored in the sympathetic neuron vesicles by the same mechanism as norepinephrine and to accumulate in non-neuronal sites by a nonspecific uptake mechanism (*8–13*). To date, MIBG has been used in various physiologic and pathologic states to determine cardiac adrenergic activity (*14–19*). Higher MIBG uptake is seen in cases of dilated cardiomyopathy than normal controls but the opposite is seen in patients with toxic cardiomyopathy following doxorubicin therapy. In both cases, the washout rate of MIBG is faster than that in controls (*3,4,20,21*). The MIBG uptake and washout patterns in patients undergoing hemodialysis and in vasospastic angina patients have not yet been established.

To date, most MIBG studies have been based on static images and SPECT data. In the present study, we obtained both dynamic and static images, created new parameters and compared and correlated these parameters with each other to distinguish the characteristics between the various cardiac disorders.

MATERIALS AND METHODS

Patients

To establish the usefulness of parameters derived from both dynamic and static studies, five groups of patients were selected: normal controls, patients undergoing hemodialysis, patients with dilated cardiomyopathy, patients who had doxorubicin therapy or patients with vasospastic angina.

Control Group. This group consisted of 15 subjects (7 men, 8 women, age 56 ± 12 yr) both patients and volunteers, who had no cardiac symptoms. None of the subjects had hypertension or diabetes mellitus and all showed normal left ventricular function on echocardiography. Six of the 15 subjects had normal coronary angiographic results. Five subjects had ^{201}Tl scintigraphy for vague complaints and showed good perfusion on stress and redistribution images.

Hemodialysis Group. All hemodialysis patients (11 men, 9 women, age 54 ± 12 yr) underwent hemodialysis for renal failure.

Received Jun. 17, 1994; revision accepted Jan. 3, 1995.

For correspondence or reprints contact: Kiyoshi Koizumi, MD, Department of Radiology, Yamanashi Medical University, Tamaho-cho, Nakakoma-gun, Yamanashi-ken-409-38, Japan.

Only those patients who had normal ^{201}Tl perfusion scans and/or those who did not show any symptoms or ECG abnormality related to ischemic heart diseases were included. All patients had hypertension, and Holter ECG monitoring showed a decreased value of R-R_{50}.

Dilated Cardiomyopathy Group. The patients in this group (5 men, 2 women, age 57 ± 13 yr) were diagnosed clinically. Echocardiography, ventriculography and coronary angiography showed dilated heart with low left ventricular ejection fractions (LVEFs) and global hypokinesia in all patients.

Doxorubicin Therapy Group. These patients (4 men, 3 women, age 38 ± 12 yr) were undergoing chemotherapy (doxorubicin) for malignant lymphoma. The study was performed at least 2 wk after chemotherapy. Doses of doxorubicin ranged between 158–342 mg/m^2 body surface area. All patients had normal ^{201}Tl perfusion scans. All patients except one had normal LVEFs determined by ECG at the time of the MIBG study. This patient, a woman with an ECG abnormality and low LVEF before doxorubicin therapy, showed no substantial change after therapy during the MIBG study.

Vasospastic Angina Group. These patients (5 men, 4 women, 61 ± 10 yr) had symptoms of coronary spasm of differing durations and an abnormality elicited by acetylcholine administration during coronary angiography. None of the patients had a coronary arterial stenosis greater than 50% and their angiographic results of left ventriculograms were normal.

Data Acquisition

Protocol. All patient groups and the normal controls, remained on their normal diets and drug regimens except for drugs that cause alterations in sympathetic activity. Drug withdrawal was carried out according to each patient's condition, but usually angiotensin-converting enzyme inhibitors, calcium antagonists, nitrates and beta-blockers were stopped 48 hr before the study. After placing the patient directly under a GCA-601E gamma camera interfaced to a GMS-55U Toshiba minicomputer Tokyo, Japan, 111 MBq [^{123}I]meta-iodobenzylguanidine (MIBG) (1.1–3.7 MBq/μg of MIBG, Daiichi Radioisotope Laboratories Ltd., Japan) was injected into the antecubital vein, and dynamic images, 1 frame/sec for 2 min and 1 frame/6 sec for the next 30 min, were acquired using a 64 × 64 matrix format. Soon after dynamic acquisition, early static planar images at anterior and left anterior oblique 45° angles were acquired using a 512 × 512 matrix format for 1 min; the standard 180° SPECT data were acquired using 36 steps at 40 s/step in a 64 × 64 matrix format. Delayed static planar images and SPECT data were also acquired approximately 4 hr after injection.

Net Injection Dose (ID) Calculation. Preinjection and postinjection syringes were counted under standardized conditions by the same gamma camera in a 512 × 512 matrix format for 1 min. The dose was calculated as follows: ID (in cpm) = preinjection syringe counts − postinjection syringe counts × decay factor.

From the calculated dose, IDs at various time intervals were corrected by multiplying the decay factors at the respective times.

Data Analysis

A time-activity curve was created from the dynamic images by drawing a ROI over the heart, excluding the lung and liver fields. The heart ROI was drawn after merging 10–50 (usually 20) late images that clearly delineated the heart, lung and liver. We did not attempt to subtract background activity from the ROIs over the heart in either the dynamic or static image phases. From the time-activity curve, the following parameters were created:

heart uptake ratio at 3 min =

$$\frac{\int_3^4 \text{Ct/dt}}{\text{Decay-corrected ID at 3 min}} \times 100\ (\%); \qquad \text{Eq. 1}$$

heart uptake ratio at 30 min =

$$\frac{\int_{30}^{31} \text{Ct/dt}}{\text{Decay-corrected ID at 30 min}} \times 100\ (\%), \qquad \text{Eq. 2}$$

where Ct = time-activity curve of the heart and ID = injected dose.

If we assume the clearance of the radionuclide from the heart to be monoexponential between time 1 (Eq. 1) and time 2 (Eq. 2), the following equation would be written:

$$A_2 = A_1 \times e^{-Kt}, \qquad \text{Eq. 3}$$

where A_2 = activity in the heart at time 2, A_1 = activity in the heart at time 1, K = clearance rate and t = duration between the time 1 and time 2. From the formula above, the following conclusions can be drawn:

$$-Kt = \ln A_2 - \ln A_1$$

$$\text{and} \quad K = \frac{\ln A_1 - \ln A_2}{t}. \qquad \text{Eq. 4}$$

Therefore,

$$\text{early clearance rate } (K_e/\text{hr}) = \frac{\ln \text{HU3} - \ln \text{HU30}}{(30-3)/60}, \qquad \text{Eq. 5}$$

where HU3 = heart uptake ratio at 3 min and HU30 = heart uptake ratio at 30 min.

A ROI over the heart was drawn on the anterior view of both early and delayed static images and total counts and pixel numbers were noted. The following parameters could be calculated from the static images:

$$\text{Early uptake} = \frac{\text{Total counts over heart in early static image}}{\text{Decay-corrected ID at early static study}} \times 100\ (\%). \qquad \text{Eq. 6}$$

$$\text{Delayed uptake} = \frac{\text{Total counts over heart in delayed static image}}{\text{Decay-corrected ID at delayed static study}} \times 100\ (\%). \qquad \text{Eq. 7}$$

By using the clearance formula above, the delayed clearance rate K_d was calculated as follows:

$$\text{Delayed clearance rate } (K_d/\text{hr}) = \frac{\ln \text{EUP} - \ln \text{DUP}}{(\text{TD} - \text{TE})/60}, \qquad \text{Eq. 8}$$

where EUP = early uptake ratio, DUP = delayed uptake ratio, TD = time at delayed static image and TE = time at early static image.

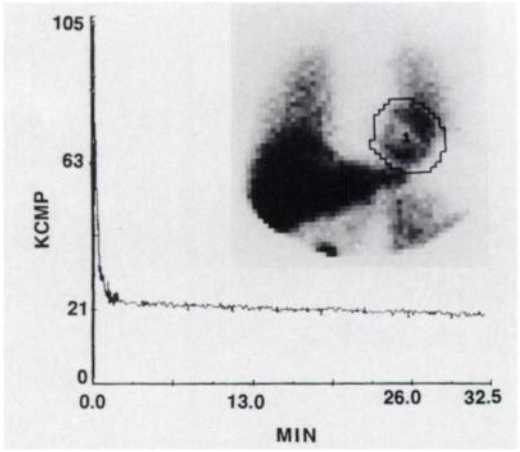

FIGURE 1. The time-activity curve created from the dynamic study by drawing a ROI over the heart. Myocardial and blood-pool activity stabilized within 2–3 min and decreased gradually thereafter.

After all data were acquired, we compared and correlated the parameters of the dynamic studies with early and delayed static studies; in seeking disparities between the two sets of parameters, we tried to determine the usefulness of the dynamic parameters in various cardiac disease processes. Statistical data were expressed as the mean + 1 s.d. and were analyzed by Student's t-test.

RESULTS

Figure 1 shows a representative time-activity curve created from the dynamic study. The curve showed that myocardial activity and blood pool stabilized within 2–3 min and decreased gradually thereafter. The mean values of heart uptake ratio at 3 min in different groups as well as the significance of differences are shown in Figure 2A. Patients with dilated cardiomyopathy showed the highest and those who had doxorubicin therapy showed the lowest heart uptake ratio at 3 min. The mean values of heart uptake ratios at 30 min and the significance of differences among the groups are shown in Figure 2B. Though the difference was not significant, the value of heart uptake ratios at 30 min in patients undergoing hemodialysis was higher than that of patients with dilated cardiomyopathy; patients who had doxorubicin therapy showed the lowest value.

It was expected from our protocol that early uptake ratios and heart uptake ratios at 30 min would correlate well, but due to differences in ROI sizes caused by different matrix sizes during acquisition, there was a small decrease in the correlation coefficient ($r = 0.925$, $n = 58$) (Fig. 3). The mean values of early uptake ratios and the significance of differences among the groups are shown in Figure 4A. The values were similar to those of heart uptake ratios at 30 min. The mean values of delayed uptake ratio and significance of differences among the groups are shown in Figure 4B. Patients under hemodialysis showed the highest values while those who had doxorubicin therapy showed the lowest values; there was, however, a much lower value of delayed uptake ratio in dilated cardiomyopathy, which was

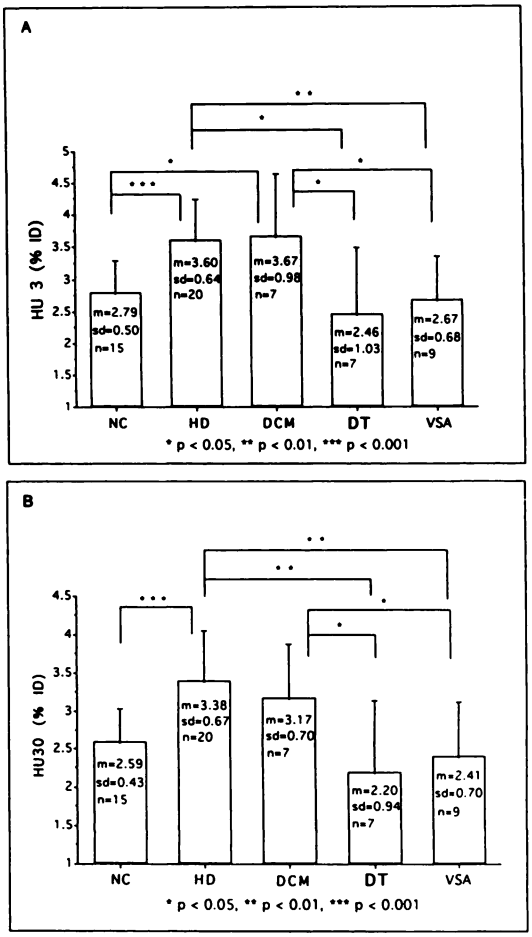

FIGURE 2. Mean and 1 s.d. for heart uptake ratio at 3 min in various groups of patients and their significant differences (A). Mean and 1 s.d. for heart uptake ratio at 30 min in the same groups and their significant differences (B).

close to the control group value. The significant differences (p value) increased between patients under hemodialysis and those with dilated cardiomyopathy, doxorubicin therapy or vasospastic angina at delayed uptake ratio compared with early uptake. The mean value of heart uptake ratios at 3 min for all groups (3.11 ± 0.84, $n = 58$) was significantly higher ($p < 0.0001$) than that of heart uptake

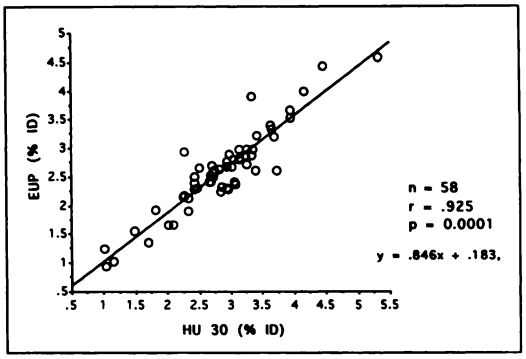

FIGURE 3. Regression curve and correlation coefficient between heart uptake ratio at 30 min (HU30) and early uptake ratio (EUP). The correlation coefficient was high ($r = 0.925$).

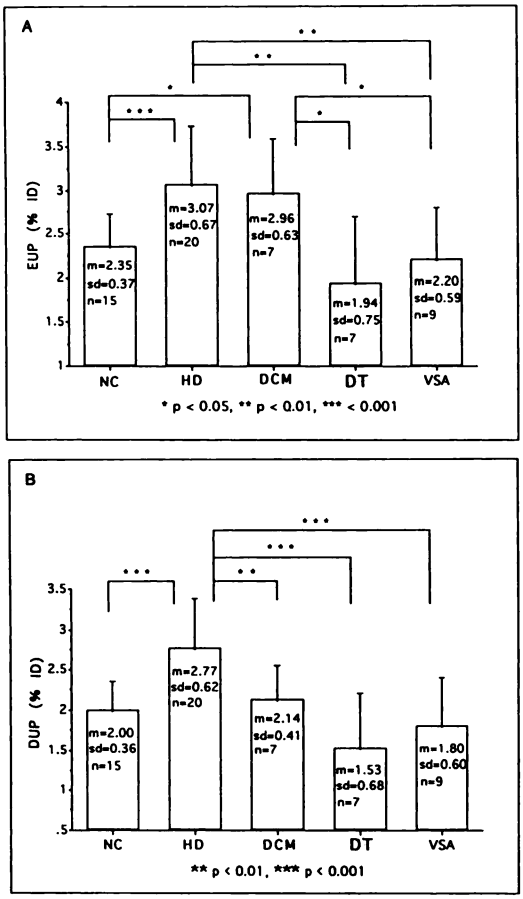

FIGURE 4. Mean, 1 s.d. and significant differences of values among all groups of patients; early uptake ratio (EUP) (A), delayed uptake ratio (DUP) (B). NC = normal controls; HD = hemodialysis; DCM = dilated cardiomyopathy; DT = doxorubicin therapy; VSA = vasospastic angina.

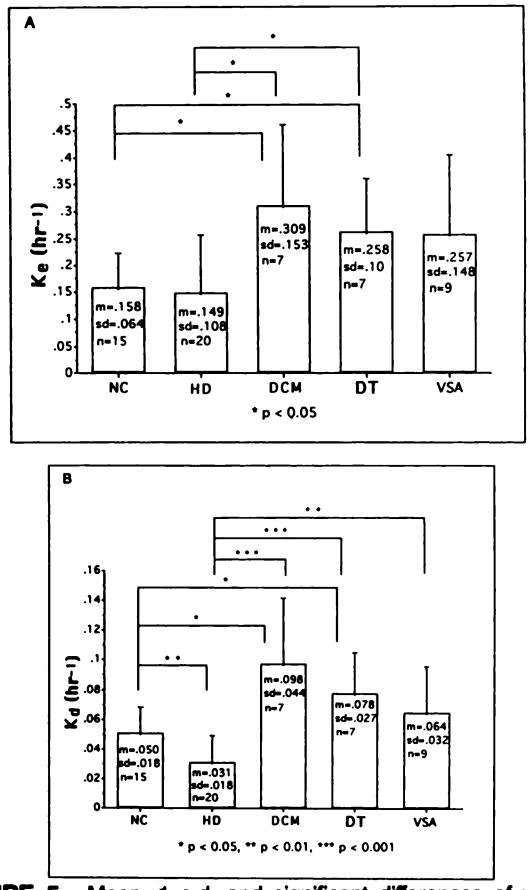

FIGURE 5. Mean, 1 s.d. and significant differences of values among all groups of patients. K_e (A) and K_d (B).

ratio at 30 min (2.86 ± 0.79), early uptake ratio (2.60 ± 0.72) and delayed uptake ratio (2.19 ± 0.69).

The mean values and significance of differences for early clearance K_e and delayed clearance K_d among the groups are shown in Figure 5. Clearance values K_e and K_d differed in each group of patients. The dilated cardiomyopathy group showed the highest and the hemodialysis group showed the lowest values of both K_e and K_d. There was a marked decrease in correlation between K_e and K_d ($r = 0.657$, $n = 0.58$) (Fig. 6), and there was a significant difference ($p < 0.0001$) between the mean values of K_e (0.201 ± 0.124, $n = 0.58$) and K_d (0.055 ± 0.034).

DISCUSSION

Although some researchers (*4,22*) have reported dynamic analysis methods, the method of acquisition was by static planar imaging at specific time intervals starting 15 min after injection; this method lacks data from early dynamic acquisition (i.e., starting from 0 min). Dae et al. (*23*) performed dynamic acquisition that started soon after injection but only in patients with transplanted hearts; from this study, no parameter measurements could be obtained. We did not subtract background activity from the ROIs over the heart in either the dynamic or static images because background subtraction, by including mediastinal or lung activity, might underestimate or overestimate real background activity, respectively.

As illustrated in the time-activity curve (Fig. 1), MIBG uptake in the heart was quick and complete and reached steady state with blood-pool activity by 2–3 min; thereafter

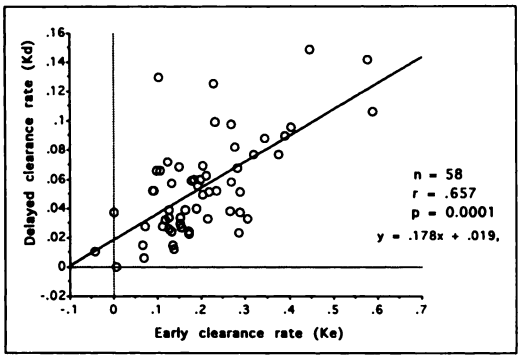

FIGURE 6. Regression curve and correlation coefficient between early clearance rate, K_e, and delayed clearance rate, K_d. There is poor correlation between the two parameters ($r = 0.657$).

MIBG started to wash out from the heart. This occurrence was reported by Glowniak et al. (*24*). The percentage of uptake at any time interval was easily calculated by taking only the integral values divided by decay-corrected injection dose at that time. In this study, heart uptake ratios at 3 min in all patient groups were always higher and significantly different ($p < 0.0001$) from other uptake parameters (heart uptake ratios at 30 min, early uptake ratio, delayed uptake ratio). To date, three different sites of MIBG accumulation have been postulated: intravesicular, extravesicular inside the neuron and non-neuronal. For our purposes, intravesicular will be referred to as vesicular and both extravesicular and non-neuronal will be combined and referred to as nonvesicular. Some researchers have (*9,21*) suggested that MIBG accumulation in sympathetic vesicles is more stable than MIBG accumulation in nonvesicular sites and remains constant for 4–6 hr; myocardial MIBG uptake determined 4 hr after injection reflects cardiac adrenergic neuron activity as well.

Other clinicians have found almost negligible uptake in transplanted and denervated hearts at 3–4 hr when none of the sympathetic neurons were intact (*16,22,23*). These findings support the hypothesis that MIBG radioactivity in the heart at 3–4 hr is almost totally due to vesicular rather than nonvesicular uptake sites. From this point of view, delayed uptake ratio may indicate only vesicular uptake at 4 hr, and heart uptake ratio at 3 min, which was higher than delayed uptake ratio, may indicate uptake in both vesicular and nonvesicular sites; therefore, the difference between the values of heart uptake ratio at 3 min and delayed uptake ratio may fairly indicate the amount accumulated in nonvesicular sites (i.e., nonvesicular uptake). We speculate that there is nonvesicular uptake at heart uptake ratios at 3 min and that the value of nonvesicular uptake is responsible for differences in clearance rates among different cardiac disorders. Therefore, heart uptake ratio at 3 min might be an important parameter to assess uptake by nonvesicular sites in various cardiac disorders in which nonvesicular uptake can in turn indicate the severity of abnormal SNS function.

A few researchers have (*11,19*) suggested that MIBG clearance is monoexponential and because they compared only the static planar images at 15–30 minutes and those at 3–4 hr. From our study, it was clear there might be at least two exponential clearance rates of MIBG, K_e and K_d, from the heart and there was a significant difference ($p < 0.001$) between them. If we consider that vesicular uptake remains constant up to a certain time (4–6 hr), rapid K_e and slow K_d might be due to uptake in two different compartments: non-neuronal and extravesicular sites of nonvesicular uptake, respectively.

By comparing the parameters in patients under hemodialysis with those in other groups, all uptake values of hemodialysis patients were significantly higher than those of other groups except for the early uptake values in patients with dilated cardiomyopathy (Fig. 2A, B; Fig. 4A, B). Differences in uptake values between hemodialysis patients and those of other groups increased with time indicating differences in nonvesicular uptake and clearance rates. The K_e and K_d of hemodialysis patients were significantly lower than those of other groups (Fig. 5A, B). The exact mechanism of higher uptake and slower clearance of MIBG in hemodialysis cases is not known, but may be explained by increased numbers of sympathetic vesicles with decreased release or by repeated uptake and release due to impairment of renal function. Increased numbers of sympathetic vesicles in the myocardium may be due to a relative increase of myocardial volume resulting from hypertrophy in patients under hemodialysis, since all of these patients were hypertensive. The Holter ECG findings in this group also suggested an increased sympathetic tone in the heart. Nakajo et al. (*9*) found that MIBG remained stable when it accumulated in vesicular rather than nonvesicular sites. The dual effect of increased numbers of vesicles and MIBG stability may account for the higher uptake in hemodialysis. Mangner et al. (*25*) showed that the kidney plays an important role in blood clearance of intact MIBG and that soon after injection, most of the urinary radioactivity is from intact MIBG. In hemodialysis patients, the diminished renal functions increased the level of serum MIBG, which may also explain the decreased washout of MIBG from nonvesicular sites.

In dilated cardiomyopathy, normal myocardium is replaced by extensive areas of interstitial and perivascular fibrosis with minimal necrosis and cellular infiltration (*26*) which may, in turn, cause the decrement of sympathetic neurons; however, an increased volume of myocardium due to dilation might cause increased uptake of MIBG in the nonvesicular sites, which may accelerate the washout. These findings are also compatible with others (*2,4,19*). The heart uptake ratio at 3 min of patients with dilated cardiomyopathy was significantly higher than that of controls or of patients with doxorubicin therapy or vasospastic angina (Fig. 2A), but no significant differences were observed in delayed uptake ratio (Fig. 4B). These contrasting findings may be explained by high nonvesicular uptake, which in turn caused rapid clearance of MIBG in patients with dilated cardiomyopathy.

Wakasugi et al. and Strashun (*21,27*) showed that cardiac toxicity of doxorubicin is dose-dependent and observed a significant difference in myocardial MIBG uptake at different dose levels when the dose crosses the threshold for cardiac toxicity. In our study, all patients received different dose levels and none showed any clinical features of cardiac toxicity; however, various stages of preclinical cardiac toxicity might be present, because we observed different uptake values in each patient ranging from 1.24% to 3.45% of injection dose at heart uptake ratios at 3 min. The heart uptake ratios at 3 min of patients with doxorubicin therapy did not significantly differ from that of controls, but was significantly lower than those of hemodialysis patients and patients with dilated cardiomyopathy. At delayed uptake ratio, differences in uptake values between

doxorubicin therapy patients and controls increased but no significant differences were observed among patients who had doxorubicin therapy, or dilated cardiomyopathy or vasospastic angina patients. These different uptake patterns might be due to higher nonvesicular uptake and more rapid clearances. Both K_e and K_d (Fig. 5A, B) of doxorubicin therapy patients were significantly higher than those of controls and patients under hemodialysis. The higher K_e and K_d values could be explained by destruction of sympathetic neurons by doxorubicin, and consequently, there was less uptake in the sympathetic vesicles, which made more MIBG available for nonspecific uptake in non-neuronal sites that promptly released MIBG. In this study, differences between heart uptake ratios at 3 min and delayed uptake ratio were proportional with the increase of total doxorubicin doses (data not shown). Therefore, both heart uptake ratios at 3 min and delayed uptake ratio in this MIBG study would be important parameters to assess nonvesicular uptake, which could possibly indicate the severity of preclinical cardiac toxicity before hand and assist the physician in calculating the dose to be administered.

Although the precise mechanism of vasospastic angina remains unknown, it was suggested that stimulation of alpha adrenoceptors, enhanced parasympathetic nervous system activity or vascular nerve lesions play an important role in developing vasospastic angina (*4,28,29,30*). Therefore, different values of our parameters were expected from controls; however, there was a marginally non-significant difference in early clearance (K_e) between these two groups ($0.05 < p < 0.1$). By comparing all parameters of patients with vasospastic angina or other sympathetic nervous system-impaired cardiac patients such as those having dilated cardiomyopathy or doxorubicin therapy, we found no significant differences among these three groups except for heart uptake ratio at 3 min, heart uptake ratio at 30 min and early uptake ratio of dilated cardiomyopathy, which might be caused by a difference in cardiac volume in the two groups. In considering these observations, we speculate that in vasospastic angina, normal SNS activity is impaired due to either the decreased number of sympathetic neurons in the heart or a hyperactive PSNS that causes similar findings with other SNS-impaired cardiac diseases.

CONCLUSION

Parameters of both dynamic and static MIBG studies could provide valuable information regarding the sympathetic functional state of the heart. Heart uptake ratios at 3 min and delayed uptake ratio calculated by dynamic and static studies are helpful for elucidating nonvesicular site uptake, which reflects the severity of SNS abnormality in the heart.

REFERENCES

1. Bhagat BD. Actions of norepinephrine, epinephrine and other amines on the cardiovascular system. In: Bhagat BD, ed. *Role of catecholamines in cardiovascular diseases*. Chicago: Charles C. Thomas; 1974:118–124.
2. Taki J, Nakajima K, Bunko H, Simizu M, Muramori A, Hisada K. Whole-body distribution of iodine-123 metaiodobenzylguanidine in hypertrophic cardiomyopathy: significance of its washout from heart. *Eur J Nucl Med* 1990;17:264–268.
3. Wakasugi S, Fischman AJ, Babich JW, et al. Metaiodobenzylguanidine: evaluation of its potential as a tracer for monitoring doxorubicin cardiomyopathy. *J Nucl Med* 1993;34:1282–1286.
4. Yamakado K, Takeda K, Kitano T, et al. Serial change of iodine-123 metaiodobenzylguanidine (MIBG) myocardial concentration in patients with dilated cardiomyopathy. *Eur J Nucl Med* 1992;19:265–270.
5. Campese VM, Romoff MS, Levitan D, Lane K, Massry SG. Mechanism of autonomic nervous system dysfunction in uremia. *Kidney Int* 1981;20:246–253.
6. Levitan D, Massry SG, Romoff M, Campese VM. Plasma catecholamines and autonomic nervous system function in patients with early renal insufficiency and hypertension: effect of clonidine. *Nephron* 1984; 36:24–29.
7. Shimizu H, Lee JD, Ogawa K, et al. Efficacy of denopamine, a B1 adrenoceptor agonist, in preventing coronary artery spasm. *Jpn Circ J* 1993;57: 175–182.
8. Tobes MC, Jaques S, Wieland DM, Sisson JC. Effect of uptake-one inhibitors on the uptake of norepinephrine and metaiodobenzylguanidine. *J Nucl Med* 1985;26:897–907.
9. Nakajo M, Shimabukuro K, Yoshimura H, et al. Iodine-131 metaiodobenzylguanidine intra- and extravesicular accumulation in rat heart. *J Nucl Med* 1986;27:84–89.
10. Sisson JC, Wieland DM, Sherman P, Mangner TJ, Tobes MC, Jacques S. Metaiodobenzylguanidine as an index of the adrenergic nervous system integrity and function. *J Nucl Med* 1987;28:1620–1624.
11. Wieland DM, Brown LE, Rogers WL, et al. Myocardial imaging with a radioiodinated norepinephrine storage analog. *J Nucl Med* 1981;22:22–31.
12. Glowniak JV, Kilty JE, Amara SG, Hoffman BJ, Turner FE. Evaluation of metaiodobenzylguanidine uptake by the norepinephrine, dopamine and serotonin transporters. *J Nucl Med* 1993;34:1140–1146.
13. Smets LA, Loesberg C, Janssen M, Metwally EA, Huiskamp R. Active uptake and extravesicular storage of miodobenzylguanidine in human neuroblastoma SK-N-SH cells. *Cancer Res* 1989;49:2941–2944.
14. Fargret D, Wolf JE, Vanzetto G, Borrel E. Myocardial uptake of metaiodobenzylguanidine in patients with left ventricular hypertrophy secondary to valvular aortic stenosis. *J Nucl Med* 1993;34:57–60.
15. Richalet JP, Merlet P, Bourguignon M, et al. MIBG scintigraphic assessment of cardiac adrenergic activity in response to altitude hypoxia. *J Nucl Med* 1990;31:34–37.
16. Gill JS, Hunter GJ, Gane G, Camm AJ. Heterogeneity of the human myocardial sympathetic innervation: in vivo demonstration by iodine-123-labeled metaiodobenzyl-guanidine scintigraphy. *Am Heart J* 1993;126:390–398.
17. Gill JS, Hunter GJ, Gane J, Ward DE, Camm AJ. Asymmetry of cardiac [^{123}I]meta-iodobenzylguanidine scans in patients with ventricular tachycardia and a "clinically normal" heart. *Br Heart J* 1993;69:6–13.
18. Katoh K, Nishimura S, Nakanishi S, Nishiyama S, Seki A, Murata H. Stunned myocardium and sympathetic denervation—clinical assessment using MIBG scintigraphy. *Jpn Circ J* 1991;55:919–922.
19. Nakajima K, Bunko H, Taki J, Shimizu M, Muramori A, Hisada K. Quantitative analysis of ^{123}I-meta-iodobenzylguanide (MIBG) uptake in hypertrophic cardiomyopathy. *Am Heart J* 1990;119:1329–1337.
20. Valdes Olmos RA, Ten Bokkel Huinink WW, Greve JC, Hoefnagel CA. Iodine-123 MIBG and serial radionuclide angiocardiography in doxorubicin-related cardiotoxicity. *Clin Nucl Med* 1992;17:163–167.
21. Wakasugi S, Wada A, Hasegawa Y, Nakano S, Shibata N. Detection of abnormal cardiac adrenergic neuron activity in adriamycin-induced cardiomyopathy with iodine-125-metaiodobenzylguanidine. *J Nucl Med* 1992;33: 208–214.
22. Rabinovitch MA, Rose CP, Schwab AJ, et al. A method of dynamic analysis of iodine-123-metaiodobenzylguanidine scintigrams in cardiac mechanical overload hypertrophy and failure. *J Nucl Med* 1993;34:589–600.
23. Dae MW, Marco TD, Botvinick EH, et al. Scintigraphic assessment of MIBG uptake in globally denervated human and canine hearts—implications for clinical studies. *J Nucl Med* 1992;33:1444–1450.
24. Glowniak JV, Wilson RA, Joyce ME, Turner FE. Evaluation of metaiodobenzylguanidine heart and lung extraction fraction by first-pass analysis in pigs. *J Nucl Med* 1992;33:716–723.
25. Mangner TJ, Tobes MC, Weiland DW, Sisson JC, Shapiro B. Metabolism

of iodine-131 metaiodobenzylguanidine in patients with metastatic phechromocytoma. *J Nucl Med* 1986;27:37–44.
26. Joshua W, Braunwald E. The cardiomyopathies and myocarditis. In: Petersdorf GR, Adams RD, Braunwald E et al., eds. *Harison's principles of internal medicine*, 10th edition. New York: McGraw-Hill; 1983: 1449–1454.
27. Strashun A. Adriamycin, congestive cardiomyopathy and meta-iodobenzylguanidine. *J Nucl Med* 1992;33:215–222.
28. Yasue H, Touyama M, Kato H, Tanaka S, Akiyama F. Prinzmetal's variant form of angina as a manifestation of alpha-adrenergic receptor-mediated coronary artery spasm: documentation by coronary arteriography. *Am Heart J* 1976;91:148–155.
29. Yasue H, Touyama M, Shimamoto M, Kato H, Tanaka S, Akiyama F. Role of autonomic nervous system in the pathogenesis of Prinzmetal's variant form of angina. *Circulation* 1974;50:534–539.
30. Kohchi K, Takebayashi S, Miyamoto AT, Nobuyoshi M. Coronary artery spasm and vascular nerve lesion. *Am Heart J* 1985;110:1071–1074.